



**HAL**  
open science

## **Cdc42 localization and cell polarity depend on membrane traffic**

Naël Osmani, Florent Peglion, Philippe Chavrier, Sandrine Etienne-Manneville

► **To cite this version:**

Naël Osmani, Florent Peglion, Philippe Chavrier, Sandrine Etienne-Manneville. Cdc42 localization and cell polarity depend on membrane traffic. *Journal of Cell Biology*, 2010, 191 (7), pp.1261-1269. 10.1083/jcb.201003091 . pasteur-03521591

**HAL Id: pasteur-03521591**

**<https://pasteur.hal.science/pasteur-03521591>**

Submitted on 11 Jan 2022

**HAL** is a multi-disciplinary open access archive for the deposit and dissemination of scientific research documents, whether they are published or not. The documents may come from teaching and research institutions in France or abroad, or from public or private research centers.

L'archive ouverte pluridisciplinaire **HAL**, est destinée au dépôt et à la diffusion de documents scientifiques de niveau recherche, publiés ou non, émanant des établissements d'enseignement et de recherche français ou étrangers, des laboratoires publics ou privés.

# Cdc42 localization and cell polarity depend on membrane traffic

Naël Osmani,<sup>1</sup> Florent Peglion,<sup>1</sup> Philippe Chavrier,<sup>2</sup> and Sandrine Etienne-Manneville<sup>1</sup>

<sup>1</sup>Cell Polarity and Migration Group, Institut Pasteur, and Centre National de la Recherche Scientifique URA 2582, 75724 Paris, Cedex 15, France

<sup>2</sup>Institut Curie and Centre National de la Recherche Scientifique UMR144, 75248 Paris, Cedex 05, France

Cell polarity is essential for cell division, cell differentiation, and most differentiated cell functions including cell migration. The small G protein Cdc42 controls cell polarity in a wide variety of cellular contexts. Although restricted localization of active Cdc42 seems to be important for its distinct functions, mechanisms responsible for the concentration of active Cdc42 at precise cortical sites are not fully understood. In this study, we show that during directed cell migration, Cdc42 accumulation at the cell leading edge relies on membrane traffic. Cdc42 and its exchange factor  $\beta$ PIX localize to

intracytoplasmic vesicles. Inhibition of Arf6-dependent membrane trafficking alters the dynamics of Cdc42-positive vesicles and abolishes the polarized recruitment of Cdc42 and  $\beta$ PIX to the leading edge. Furthermore, we show that Arf6-dependent membrane dynamics is also required for polarized recruitment of Rac and the Par6- $\alpha$ PKC polarity complex and for cell polarization. Our results demonstrate influence of membrane dynamics on the localization and activation of Cdc42 and consequently on directed cell migration.

## Introduction

Cell polarity is crucial both during development and in the adult, where it participates in polarized cell functions such as neuronal synaptic transmission, epithelial barriers, or cell migration. Cdc42 is a major regulator of cell polarity from yeast to mammalian cells (Etienne-Manneville, 2004) and controls the direction of cell migration in chemotaxis and wound-induced migration (Allen et al., 1998; Etienne-Manneville and Hall, 2001; Li et al., 2003). Cdc42 activity can be regulated either positively by guanine nucleotide exchange factors (GEFs) or negatively by GTPase-activating proteins (GAPs; Etienne-Manneville and Hall, 2002). Inhibition but also constitutive activation of Cdc42 or its GEF perturbs cell orientation (Adams et al., 1990; Etienne-Manneville and Hall, 2001; Caviston et al., 2002; Etienne-Manneville, 2004), indicating that Cdc42 activation must be temporally and spatially restricted to successfully promote cell polarization (Park and Bi, 2007). In *Saccharomyces cerevisiae*, Cdc42 accumulates at the presumptive growth site, where it promotes polarized cell growth (Nern and Arkowitz, 2000) or the formation of mating projection in response to

pheromone (Johnson, 1999). During wound-induced directed cell migration, Cdc42 is recruited to the wound edge to induce the polarization of the cell toward the wound (Nobes and Marsh, 2000; Etienne-Manneville and Hall, 2001; Palazzo et al., 2001; Nalbant et al., 2004).

The mechanisms that control Cdc42 localization are likely to be crucial for cell polarity but are still poorly understood. In budding yeast, Cdc42p-restricted localization requires the polarized recruitment of the Cdc42p GEF Cdc24p, which is regulated by various polarity cues (Nern and Arkowitz, 2000; Shimada et al., 2000). It also involves actin-driven membrane delivery (Wedlich-Soldner et al., 2003; Slaughter et al., 2009). In migrating astrocytes, Cdc42 recruitment and activation to the leading edge depend on its GEF  $\beta$ PIX (Osmani et al., 2006), but the involvement of membrane trafficking in Cdc42 localization and cell polarity remains unknown. Thus, we investigated the dynamics of Cdc42 and its regulation in polarizing astrocytes. The colocalization of Cdc42 with Arf6, a key regulator of membrane endocytosis and recycling, prompted us to study the role

Correspondence to Sandrine Etienne-Manneville: sandrine.etienne-manneville@pasteur.fr

Abbreviations used in this paper: APC, adenomatous polyposis coli; CCD, charge-coupled device; GAP, GTPase-activating protein; GEF, guanine nucleotide exchange factor.

© 2010 Osmani et al. This article is distributed under the terms of an Attribution-Noncommercial-Share Alike-No Mirror Sites license for the first six months after the publication date [see <http://www.rupress.org/terms>]. After six months it is available under a Creative Commons License [Attribution-Noncommercial-Share Alike 3.0 Unported license, as described at <http://creativecommons.org/licenses/by-nc-sa/3.0/>].

of Arf6-dependent membrane traffic in Cdc42 localization and cell polarity.

Arf6 is a member of the ARF (ADP ribosylation factor) family of small GTPases. Arf6 localizes at the plasma membrane and the endocytic system, where it acts in a wide range of processes, including endocytosis, recycling, and organization of the actin cytoskeleton (D'Souza-Schorey and Chavrier, 2006). Arf6 is overexpressed in invasive tumors like gliomas and is essential for tumor cell invasion (Sabe, 2003; Li et al., 2006; Hu et al., 2009). Arf6 function in cell migration (Santy and Casanova, 2001; Svensson et al., 2008) is thought to be mediated by its role in the regulation of the Rho GTPase Rac and actin remodeling (Di Cesare et al., 2000; Matafora et al., 2001; Palacios and D'Souza-Schorey, 2003; Cotton et al., 2007). In this study, we show that Arf6 also plays a key role in the regulation of Cdc42 and cell polarity.

## Results and discussion

We used a wound-induced astrocyte migration assay to monitor the dynamics of GFP-Cdc42 during cell polarization (Fig. 1 and Videos 1 and 2). Although expression of GFP alone induced a diffuse fluorescence that concentrated in the nucleus, GFP-Cdc42 accumulated at the leading edge of wound-edge cells (Fig. 1 A). We have previously demonstrated that the increased GFP-Cdc42 fluorescence at the leading edge was not caused by membrane ruffling but reflected the local accumulation of Cdc42 at the leading edge (Etienne-Manneville and Hall, 2001; Osmani et al., 2006). Cdc42-GFP was also visible in limited regions of cell-cell contact, as reported previously (Michaelson et al., 2001). In addition, Cdc42 was visible on a perinuclear compartment, where it colocalized with the cis-Golgi marker GM130 (Fig. 1 E), which is in agreement with the previously reported interaction of Cdc42 with the  $\gamma$ COP subunit of coatomer (Erickson et al., 1996; Wu et al., 2000; Nalbant et al., 2004). Cdc42 also labeled vesicles of various sizes. In nonmigrating confluent cells, Cdc42-positive vesicles were mainly immobile (Fig. 1 B and Video 3). In migrating astrocytes, large Cdc42-positive structures were visible and resembled macropinosomes, which form during astrocyte migration (Video 4). These large vesicles tended to accumulate when Cdc42 was largely overexpressed (Video 2), possibly as a consequence of Cdc42 function in endocytosis (Georgiou et al., 2008; Rodal et al., 2008; Hehnyly et al., 2009). In migrating cells, we also observed small and very dynamic Cdc42-positive vesicles, moving in a directed manner toward the leading edge and also from the leading edge toward the cell center (Fig. 1 C and Videos 1 and 2). To determine the nature of the Cdc42-positive membrane structures, we stained cells with the early endosome marker EEA1. Large and some of the small Cdc42-positive vesicles were EEA1 positive, showing the localization of Cdc42 on the endosomal compartment (Fig. 1 F).

The presence of EEA1 on Cdc42-positive vesicles led us to compare the localization of Cdc42 with that of Arf6, a well-established component of endocytic and recycling pathways (D'Souza-Schorey and Chavrier, 2006). Arf6 has been shown to control the vesicular traffic of the Rho GTPase Rac1

(Albertinazzi et al., 2003; Balasubramanian et al., 2007; Cotton et al., 2007), but its relationship with Cdc42 has not been investigated so far. In the absence of antibody suitable for immunofluorescence, we used a CFP-tagged Arf6 construct. CFP-Arf6 localized at the plasma membrane and decorated intracellular vesicles in cell periphery and in a pericentriolar region (Peters et al., 1995; Radhakrishna and Donaldson, 1997; D'Souza-Schorey et al., 1998). CFP-Arf6 colocalized with Cdc42 on patches at the plasma membrane and on intracytoplasmic vesicles (Fig. 2, A and B). We depleted Arf6 using two different siRNA (Fig. S1) and analyzed the dynamics of GFP-Cdc42-positive structures (Video 5). In Arf6-depleted cells, the Golgi localization of Cdc42 was perturbed, although the Golgi structure, as seen with GM130 staining, remained intact (Fig. S1 B). Cdc42 localization on vesicles was only slightly decreased, and Cdc42-GFP was still present on EEA1-positive vesicles, which often accumulated in a perinuclear area (Fig. 2 C and Fig. S1 C). Rab5 inhibition was more potent than Arf6 in perturbing Cdc42 localization on vesicles (Fig. 2 C), suggesting that Cdc42 localization on vesicles requires endocytosis and that Arf6 does not play a major role in this process. Nevertheless, depletion of Arf6 dramatically reduced the dynamics of the Cdc42-positive vesicles (Fig. 2 D and Video 2). These results indicate that endocytosis and Arf6-dependent membrane traffic are key regulators of membrane-bound Cdc42 dynamics in migrating cells.

We then tested whether Cdc42-polarized recruitment required membrane traffic. Inhibition of Arf6 by siRNA or by a dominant-negative construct dramatically perturbed Cdc42 recruitment at the leading edge (Fig. 2, E and F). Similarly, dominant-negative Rab5 prevented Cdc42 accumulation at the leading edge (Fig. 2 E). In contrast, control siRNA (Fig. 2, E and F, siCTL) and siRNA-mediated depletion of Rac, which prevents astrocyte migration but not centrosome reorientation (Etienne-Manneville and Hall, 2001), had no effect (Fig. S2). These observations show that Cdc42 accumulation at the leading edge plasma membrane involves Arf6-dependent vesicular traffic independently of the role of Arf6 in the regulation of Rac activity and cell motility. They suggest that recycling of membrane-bound Cdc42 is involved in Cdc42 recruitment to sites of cell polarization. A similar role of membrane recycling has been suggested for polarized recruitment of Cdc42 to the bud site in *S. cerevisiae* (Wedlich-Soldner et al., 2003; Slaughter et al., 2009), suggesting that membrane traffic may be a very general mechanism to direct the delivery of Cdc42 to polarizing sites.

We then determined whether vesicular traffic was involved in wound-induced Cdc42 activation. In response to the scratch, Cdc42 is activated by the exchange factor  $\beta$ PIX downstream of an integrin-induced Src-dependent signaling cascade, which is activated at the cell wound edge (see Fig. 5; Osmani et al., 2006). Depletion of Arf6 abolished wound-induced Cdc42 activation (Fig. 3 A), demonstrating the role of Arf6-dependent membrane dynamics in Cdc42 regulation. In agreement with the role of Arf6 in focal adhesion turnover (Daher et al., 2008; Torii et al., 2010), focal adhesions appeared longer in Arf6-depleted than control cells. However, the distribution of focal adhesions remained polarized (Fig. S1 D), indicating that in Arf6-depleted and control cells, integrin

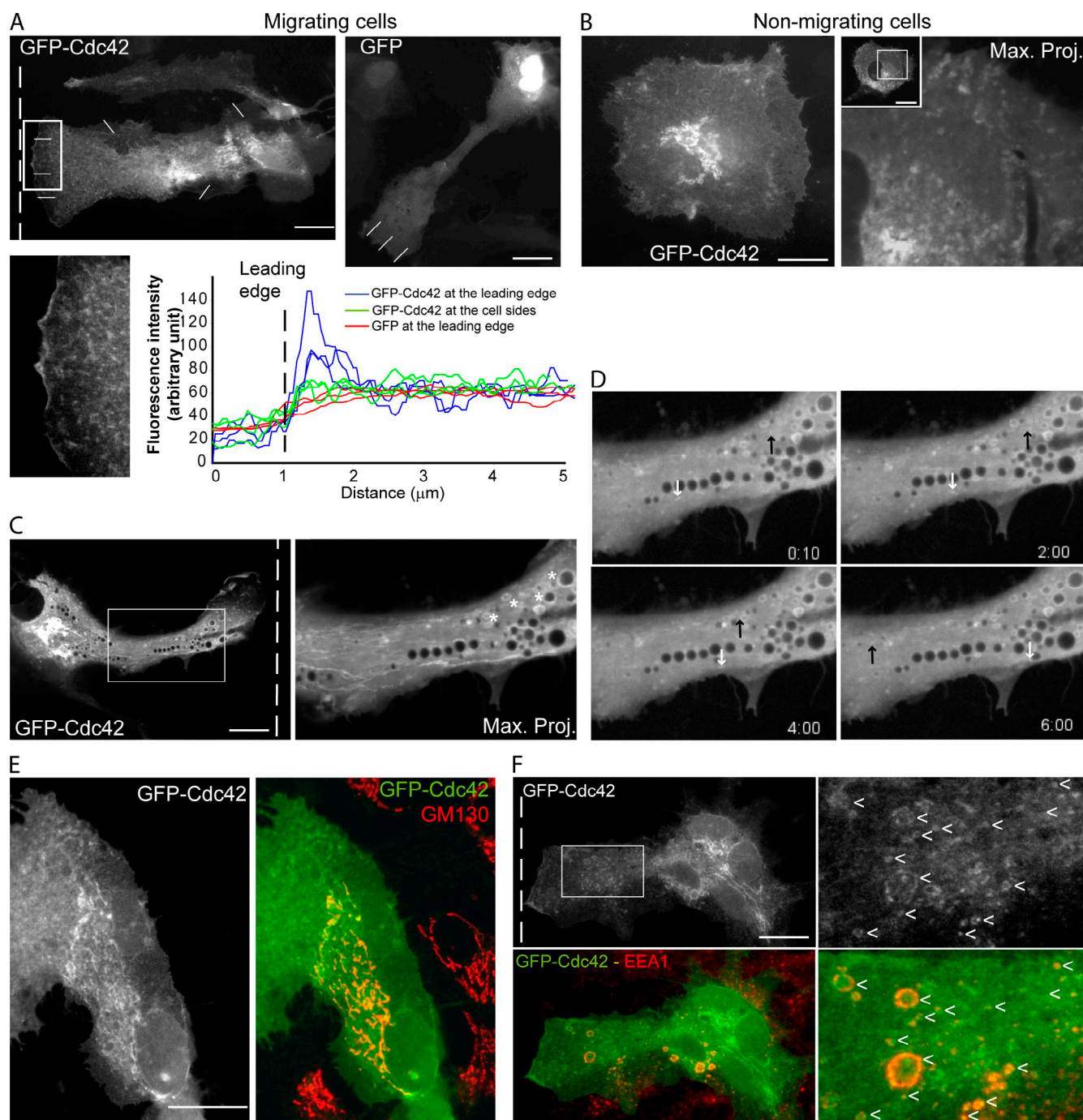


**Figure 1. GFP-Cdc42 localizes to plasma membrane and intracellular vesicles of migrating cells.** (A) GFP-Cdc42 (top left) and GFP (top right) fluorescence in migrating primary astrocytes. (bottom left) Higher magnification view of the boxed region shows accumulation of GFP-Cdc42 at the leading edge. (bottom right) Fluorescence intensity of GFP-Cdc42 (blue) measured along three lines (as indicated) drawn across the leading edge (blue) or side edge (green) is shown. Fluorescence intensity of GFP measured along three lines drawn across the leading edge of the GFP-expressing cell is shown in red. Cell-cell contact areas with increased Cdc42 intensity have been disregarded. (B) GFP-Cdc42 fluorescence in a nonmigrating confluent astrocyte (left) and image showing the maximum projection of [Video 3](#) (right). (C) Images showing the maximum projection of [Video 2](#). A higher magnification of the boxed area is shown on the right. Directed movement of small Cdc42-positive vesicles appears as white lines along the length of the protrusion. Large immobile Cdc42-positive vesicles are indicated with asterisks. (D) Still images from [Video 2](#) showing the retrograde (black arrow) and anterograde movement (white arrows) of Cdc42-positive vesicles in the cell protrusion. (E) GM130 staining (red) in GFP-Cdc42 (green)-expressing cells. (F) EEA1 staining (red) in GFP-Cdc42 (green)-expressing cells showing the endosomal EEA1 marker on Cdc42-positive vesicles (arrowheads). Images are representative of at least 100 cells from three independent experiments. The dashed line indicates the direction of the wound. Bars, 10  $\mu\text{m}$ .

signaling was restricted to the wound edge. In migrating cells,  $\beta$ PIX colocalized with Cdc42 at the leading edge (Fig. 3, B and C) and on small intracytoplasmic vesicles (Fig. 3 C,

arrowheads), but it was absent from larger cytoplasmic structures (Fig. 3 C, asterisk).  $\beta$ PIX recruitment to the leading edge was strongly reduced in Arf6-depleted cells (Fig. 3 D), suggesting

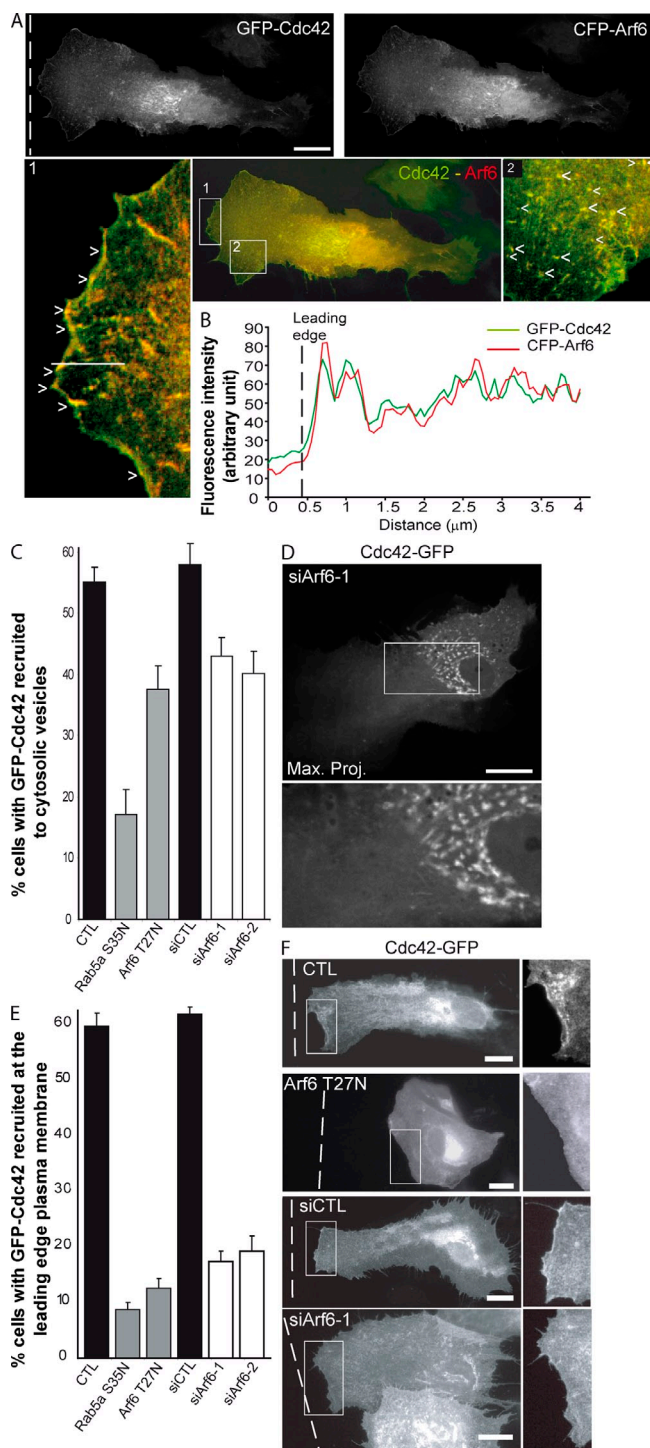


**Figure 2. Arf6 colocalizes with Cdc42 and regulates Cdc42 dynamics and localization.** (A) Colocalization of GFP-Cdc42 (green) and CFP-Arf6 (red) in a migrating astrocyte. Higher magnification images of boxed areas 1 and 2 are shown on the left and right, respectively. CFP-Arf6 and GFP-Cdc42 colocalized (arrowheads) in discrete areas at the leading edge plasma membrane (box 1) and on intracellular vesicles (box 2). (B) Fluorescence intensities of GFP-Cdc42 (green) and CFP-Arf6 (red) measured along the line shown in A (box 1). (C) GFP-Cdc42 recruitment to intracytoplasmic vesicles in astrocytes microinjected with the indicated constructs or nucleofected with the indicated siRNA. (D) Maximum projection of Video 4. (bottom) A higher magnification of the boxed area is shown. (E) Recruitment of GFP-Cdc42 to the leading edge of migrating astrocytes after microinjection with the indicated constructs or nucleofection with the indicated siRNA. (F) GFP-Cdc42 fluorescence images in cells microinjected with the indicated

that vesicular traffic controls the delivery of Cdc42 together with its GEF  $\beta$ PIX to the wound-edge plasma membrane (see Fig. 5). It is tempting to speculate that wound-induced Src activation downstream of integrins and interaction with Scrib promotes  $\beta$ PIX activation and consequently Cdc42 activation (see Fig. 5; Feng et al., 2006; Osmani et al., 2006). Active Cdc42 together with  $\beta$ PIX may inhibit Arf6 activity at the leading edge via GIT, a  $\beta$ PIX-associated Arf6 GAP (Hoefen and Berk, 2006), to maintain a stable accumulation of Cdc42 at the leading edge of migrating cells. Alternatively, Cdc42 may also modulate Arf6 activity through aPKC and GSK3 $\beta$  as shown in epithelial cells (Farooqui et al., 2006).

In migrating astrocytes, Cdc42 controls centrosome positioning in front of the nucleus and cell orientation toward the wound (Etienne-Manneville and Hall, 2001). Wound-induced Cdc42 activation induces the recruitment and activation of the polarity protein complex Par6–aPKC, which in turn phosphorylates GSK3 $\beta$  to locally promote adenomatous polyposis coli (APC) clustering at microtubule plus ends, microtubule anchoring, and centrosome reorientation (Etienne-Manneville and Hall, 2003; Etienne-Manneville et al., 2005; Manneville et al., 2010). Depletion of Arf6 strongly affected the Cdc42-dependent recruitment of Par6 and aPKC to the wound edge of the cells (Fig. 4 A). Immunolocalization of the Thr410-phosphorylated aPKC indicated that the leading edge recruitment of the activated aPKC also depended on Arf6 (Fig. 4 B). APC accumulation at microtubule plus ends was strongly reduced in Arf6-depleted cells (Fig. 4 C). These results confirm the role of Arf6-dependent membrane traffic in the wound-induced activation of Cdc42- and Cdc42-dependent polarity pathway. Consistently, inhibition of Arf6 by siRNA or a dominant-negative construct inhibited centrosome and Golgi reorientation in wounded astrocytes (Fig. 4, D and E). Expression of an siRNA-insensitive Arf6 construct restored a correct cell orientation (Fig. 4 E). Expression of a GFP protein or transfection with control siRNA had no effect on cell polarization. Thus, we conclude that the regulation of Cdc42 localization by Arf6 contributes to the activation of the Par6–aPKC polarity pathway and to the polarized reorganization of the microtubule network (Fig. 5). Dominant-negative Rab5 and Eps15, which interfere with endocytosis, also prevented Cdc42 recruitment to the leading edge and inhibited cell orientation (Fig. 2 E and not depicted). Collectively, these observations indicate that membrane traffic is involved in the regulation of cell polarity by controlling Cdc42-polarized delivery to cortical sites and consequently by promoting the integrin-mediated activation of Cdc42 and the Cdc42-mediated polarity pathway (Fig. 5).

In addition to its role in cell orientation, Arf6-dependent membrane traffic also controlled the formation of protrusion (Fig. 4 F). We have shown previously that protrusion length depends essentially on Rac activity (Etienne-Manneville and

constructs or nucleofected with the indicated siRNA. (right) Higher magnification images of the leading edges (boxed areas) are shown. Dotted lines indicate the direction of the wound. Data are shown as mean  $\pm$  SEM of three to six independent experiments totaling >200 cells. Bars, 10  $\mu$ m.

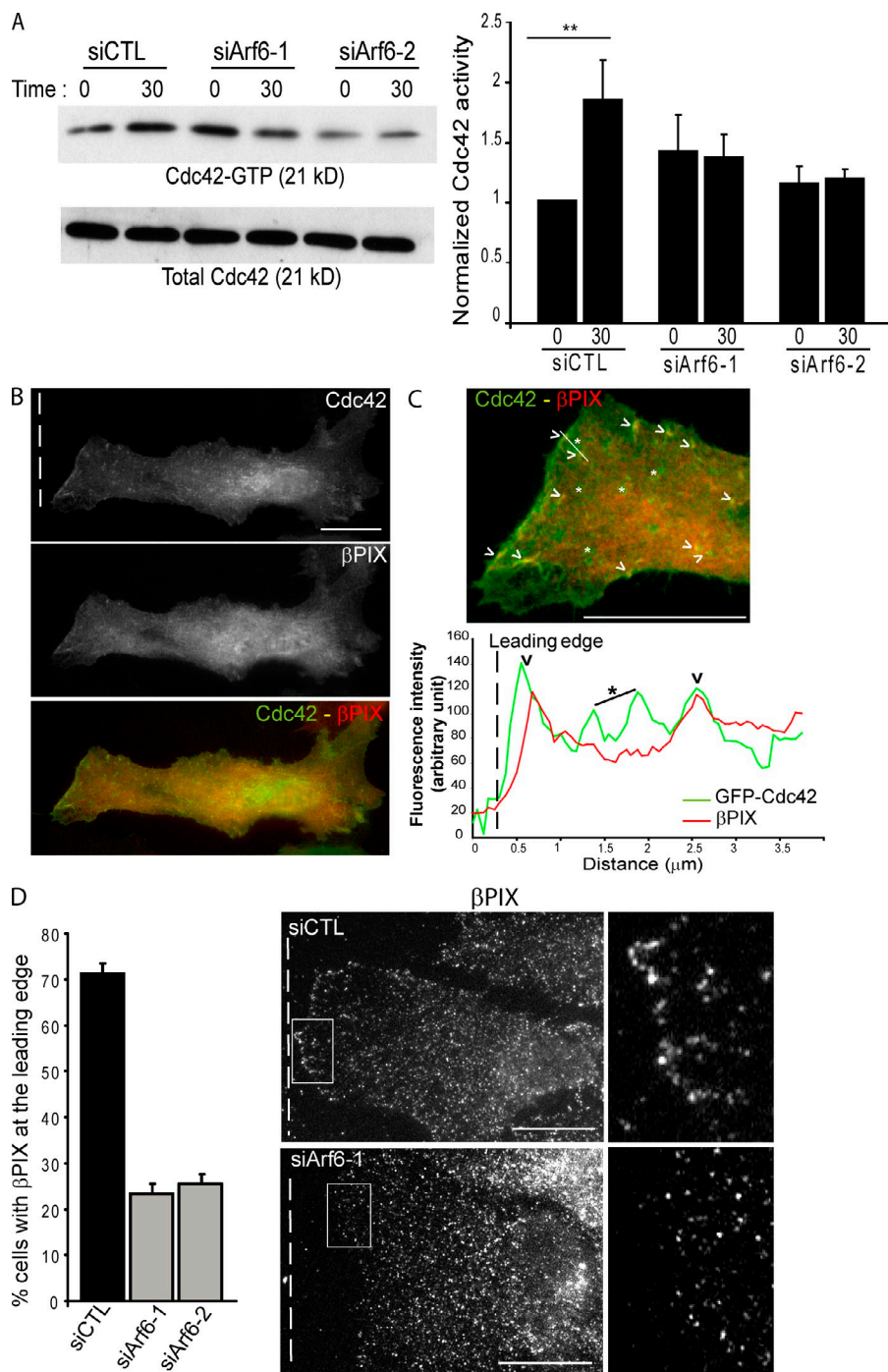
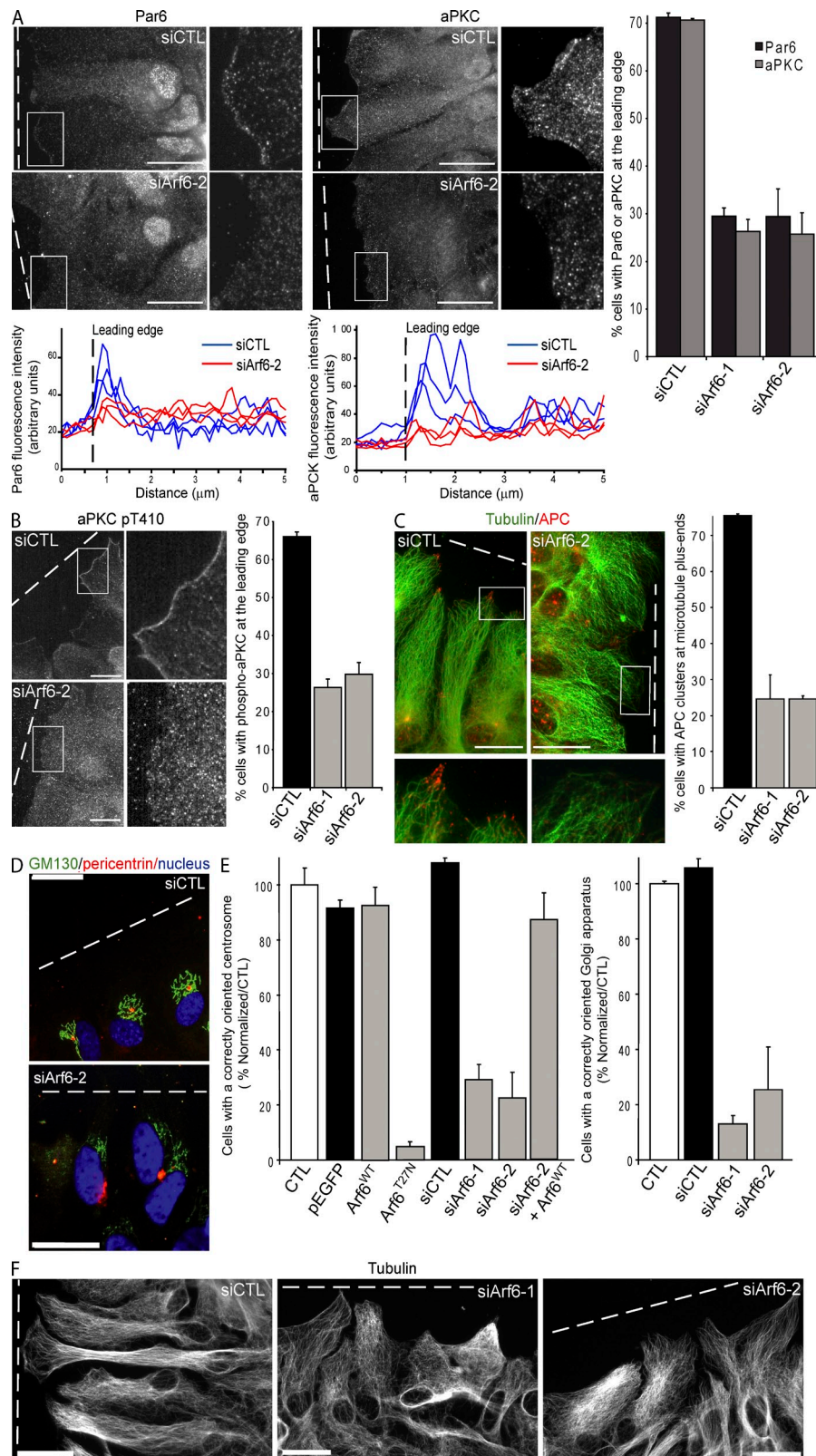


**Figure 3. Arf6 controls the localization of the Cdc42-GEF  $\beta$ PIX and Cdc42 activation upon wounding.** (A) Wound-induced Cdc42 activation in cells nucleofected with the indicated siRNA. (left) Western blots showing a representative experiment. (right) Histogram showing the quantitative measurement of Cdc42 activity. Values are normalized by the Cdc42 activity observed in the control condition (siCTL, time 0). \*\*,  $P = 0.01$ . (B) Colocalization of GFP-Cdc42 (green) and HA- $\beta$ PIX (red) in a migrating astrocyte. (C) Magnified view of the front edge area of the cell shown in B. Arrowheads point to regions showing colocalization of GFP-Cdc42 and HA- $\beta$ PIX. Fluorescence intensities of GFP-Cdc42 (green) and HA- $\beta$ PIX (red) along the line drawn in the image show the colocalization of Cdc42 and  $\beta$ PIX at the leading edge and on some of the Cdc42-positive vesicles. Large Cdc42-positive vesicles (asterisks) are usually not stained with the anti- $\beta$ PIX antibody. (D)  $\beta$ PIX recruitment to the leading edge of astrocytes nucleofected with the indicated siRNA. (left) The percentage of cells with a leading edge accumulation of  $\beta$ PIX. (right) Representative images of  $\beta$ PIX immunofluorescence in cells nucleofected with the indicated siRNA. Higher magnification views of the boxed regions are shown. Dotted lines indicate the direction of the wound. Data are shown as mean  $\pm$  SEM of three independent experiments totalizing >300 cells. Bars, 10  $\mu$ m.

Hall, 2001). However, although Rac depletion totally abolished astrocyte protrusion and migration, Arf6 depletion only had a moderate effect. Protrusions in Arf6-depleted cells were shorter (Figs. 2 F and 4 F), and cell migration was 20–25% slower than in control cells (Fig. S1 E and Videos 6 and 7). We found that Arf6 and  $\beta$ PIX were required for Rac accumulation at the leading edge of migrating astrocytes (Fig. S3). However, in contrast with Cdc42 (Osmani et al., 2006), Rac recruitment did not involve  $\beta$ PIX catalytic activity but required the SH3 domain of  $\beta$ PIX (Fig. S3; Cau and Hall, 2005; Mott et al., 2005; ten Klooster et al., 2006). We could not detect any change in Rac activity levels after Arf6 depletion.

These observations suggest that, in absence of polarized recruitment to the leading edge, Rac activity, although not sufficient to promote a fully developed protrusion, can sustain cell migration. These observations suggest that Arf6-dependent vesicular traffic promotes  $\beta$ PIX accumulation at the leading edge, which is required for Cdc42 accumulation and activation and for Rac accumulation, whereas Rac activity is regulated by another GEF. Several GEFs including Tiam1 and Dock180 may be involved in Rac activation at the leading edge (Santy et al., 2005; Pegtel et al., 2007). By controlling both cell polarization via Cdc42 and cell protrusion via Rac and PAK, Arf6 emerges as a crucial regulator of

**Figure 4. Arf6 controls the Cdc42-mediated polarity signaling pathway and cell orientation during migration.** Astrocytes were nucleofected with the indicated siRNA or microinjected with the indicated constructs. (A) Immunostaining of Par6 and aPKC in migrating astrocytes 4 h after wounding. (right) Higher magnification views of the boxed regions are shown. Graphs plotting the fluorescence intensity of Par6 and aPKC measured along lines drawn perpendicularly to the leading edge of three different siCTL (blue)- and siArf6-2 (red)-transfected cells are shown below the corresponding images. Histogram showing the percentage of wound-edge cells with a leading edge accumulation of Par6 (black bars) and aPKC (gray bars). (B) Immunostaining of Thr<sup>410</sup>-phosphorylated aPKC in control or Arf6-depleted astrocytes 4 h after wounding. (right) Higher magnification views of the boxed areas are shown. The histogram shows the percentage of cells with an accumulation of phospho-aPKC at the leading edge. (C) Immunostaining of APC (red) and tubulin (green) in migrating astrocytes 8 h after wounding. (right) Histogram shows the percentage of wound-edge cells with APC clusters at microtubule plus ends. (D) Fluorescence images of the microtubules (green), centrosome (red), and nucleus (blue) in nucleofected migrating astrocytes 8 h after wounding. (E) Centrosome and Golgi reorientation 8 h after wounding. (F) Immunostaining of tubulin in migrating astrocytes 16 h after wounding. Data are shown as mean  $\pm$  SEM of three independent experiments totalizing >300 cells. The dotted lines indicate the direction of the wound. Bars, 10  $\mu$ m.



directed cell migration, further emphasizing its critical role in tumor invasion.

Collectively, our results show that membrane dynamics plays a key role in cell polarization and migration by promoting Cdc42 delivery to the leading edge of cells. Evidence is

accumulating for a role of Cdc42 in endocytosis and may support the hypothesis of a Cdc42-driven feedback loop enhancing Cdc42 accumulation at the leading edge, similar to the role of actin-based membrane delivery of Cdc42 in polarized yeast cells (Wedlich-Soldner et al., 2004).

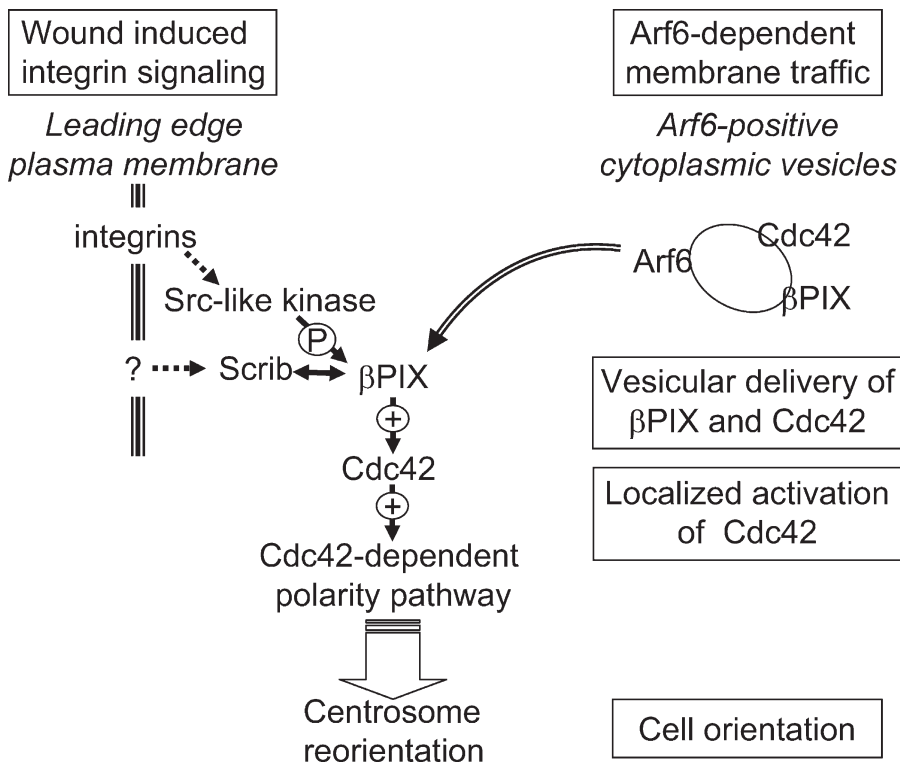


**Figure 5. Arf6-dependent membrane traffic and wound-induced integrin engagement control Cdc42 activation at the wound edge.** Cdc42 accumulation and activation at the wound edge result from wound-induced integrin signaling (Etienne-Manneville and Hall, 2001) and Arf6-dependent vesicular delivery of Cdc42 and its GEF  $\beta$ PIX. We propose that  $\beta$ PIX interaction with Scrib (Osmani et al., 2006) and phosphorylation by Src (Feng et al., 2006) at the wound edge promotes  $\beta$ PIX GEF activity toward Cdc42 and thus leads to the generation of a Cdc42-mediated polarity signal that involves Par6, aPKC, and APC (Etienne-Manneville and Hall, 2003).

## Materials and methods

### Materials

Anti- $\alpha$ -tubulin was obtained from Sigma-Aldrich, phalloidin-rhodamine from Invitrogen, anti-pericentrin from BabCO, anti-GM130, anti-EEA1, and anti-Rac1 from BD, anti-Arf6 from AbCam, anti-Cdc42, anti-Par6, and anti-PKC $\zeta$  from Santa Cruz Biotechnology, Inc., anti-PKC $\zeta$  pT410 from Cell Signaling Technology, and anti- $\beta$ PIX from Millipore. Anti-APC was provided by I. Nathke (University of Dundee, Dundee, Scotland, UK). Secondary antibodies were obtained from Jackson ImmunoResearch Laboratories, Inc. pEGFP-Cdc42,  $\beta$ PIX, and Arf6 constructs were previously described (Osmani et al., 2006). Two siRNA duplexes corresponding to rat Arf6 starting at nucleotides 76 (siArf6-2) and 143 (siArf6-1; GenBank/EMBL/DBJ accession no. NM\_024152) were obtained from Prologo. The sequence of the siArf6-2 did not match the corresponding human sequence allowing expression of a human Arf6 construct. siRNAs were introduced into cells by nucleofection according to the vendor's instructions (Lonza).

### Cell culture and scratch-induced migration

Primary rat astrocytes were prepared as described previously (Etienne-Manneville, 2006). For scratch-induced assays, cells were seeded on poly-L-ornithine-precoated coverslips or 90-mm diameter dishes and grown to confluence in MEM medium supplemented with 10% serum. Individual wounds (suitable for microinjection and immunofluorescence;  $\sim$ 300- $\mu$ m wide) were made with a microinjection needle. Wound closure occurred  $\sim$ 16–24 h later. Multiple wounds (suitable for subsequent biochemical analysis) were made with an eight-channel pipette (0.1–2- $\mu$ l tips) that was moved several times across the 90-mm dish. Nuclear microinjections in the first row of wound-edge cells were performed immediately after scratching. Expression vectors were used at 100–400  $\mu$ g/ml.

### Immunofluorescence and image quantification

Cells were stained as described previously (Etienne-Manneville, 2006). Epifluorescence images of fixed cells mounted in Mowiol (Polysciences, Inc.) were obtained on a microscope (DM6000; Leica) equipped with 40 $\times$  1.25 NA and 63 $\times$  1.4 NA objectives and were recorded on a charge-coupled device (CCD) camera (DFC350 FX; Leica) using Application Suite AF software (Leica). Images were also obtained with the fast spinning-disk confocal system (UltraView RS Nipkow-disk; PerkinElmer) equipped with 40 $\times$  1.4 NA and 63 $\times$  1.4 NA objectives and recorded on an electron-multiplying CCD camera (C-9100; Hamamatsu Photonics).

### Live cell imaging

Videos 1–7 were acquired at the Plateforme d'Imagerie Dynamique at the Pasteur Institute. Cells or nucleofected cells were seeded on 35-mm glass-bottom dishes (MaTek) and grown to confluence. The monolayer was wounded, and cells were microinjected with pEGFP-Cdc42. 6 h later, cells were imaged at 37 $^{\circ}$ C in MEM culture medium supplemented with 20 mM Hepes using either a fast spinning-disk confocal system (UltraView RS Nipkow-disk) equipped with 40 $\times$  1.4 NA and 63 $\times$  1.4 NA objectives and recorded on an electron-multiplying CCD camera (C-9100) or a CCD camera (ORCA II ER; Hamamatsu Photonics) installed on a microscope (Axiovert 200M; Carl Zeiss, Inc.) equipped with 10 $\times$  0.45 NA, 40 $\times$  1.4 NA, and 63 $\times$  1.4 NA objectives.

### Centrosome and Golgi apparatus reorientation and cell protrusion

Centrosome and Golgi apparatus reorientation was determined as previously described (Etienne-Manneville, 2006). In brief, 8 h after wounding, astrocytes were fixed and stained with anti-pericentrin (centrosome), anti-GM130 (Golgi apparatus), Hoechst (nucleus), and anti-Myc when necessary. Cells in which the centrosome was within the quadrant facing the wound ( $\pm$ 45 $^{\circ}$  deviation from the direction perpendicular to the wound) or cells in which the Golgi apparatus was within  $\pm$ 60 $^{\circ}$  from the direction perpendicular to the wound were scored as positive. For each point, at least 300 cells from three independent experiments were examined. Because random polarization is 25% for the centrosome and 33% for the Golgi apparatus in our assay, data were normalized to control conditions by subtracting random orientation (25% for centrosome reorientation or 33% for Golgi apparatus reorientation) and by setting reorientation to 100% for cells treated by a control siRNA against GFP (siGFP).

Protrusion formation was determined as described previously (Etienne-Manneville and Hall, 2001; Etienne-Manneville, 2006). In brief, 16 h after wounding, astrocytes were fixed and stained with anti- $\alpha$ -tubulin. Cells that were at least four times longer than wide were scored as positive.

### Protein localization

**Cdc42 localization.** Microinjection of GFP-tagged Cdc42 WT was used for visualization of Cdc42 because of the lack of anti-Cdc42 antibodies that work in immunofluorescence. The percentage of cells showing an increased GFP fluorescence at the leading edge was determined 4 h after wounding (unless otherwise stated).

**$\beta$ PIX, Par6, or aPKC localization.** 4 h after wounding, cells were fixed and stained with the appropriate antibody. For the scoring of polarized protein recruitment, cells in which the protein was specifically enriched at

the leading edge were counted as positive. Relative fluorescence intensity was measured at the leading edge using ImageJ software (National Institutes of Health) in three different cells from three independent experiments. In the case of GFP-Cdc42, fluorescence intensity was measured in three different areas of the same cell leading edge.

In general, only very few migrating astrocytes show membrane ruffling at the leading edge. However, to avoid artifacts from increased fluorescence caused by membrane ruffling, these cells were not included in the analysis.

**APC localization.** 8 h after wounding, cells were fixed and stained with APC and tubulin antibodies. The percentage of cells showing APC clusters at microtubule tips of the leading edge was measured.

### Cdc42 activity

Cells were washed with ice-cold PBS and lysed at 4°C in RIPA buffer (10 mM Tris-HCl, pH 7.5, 150 mM NaCl, 0.5% sodium deoxycholate, 0.1% SDS, 10 mM MgCl<sub>2</sub>, 1 mM orthovanadate, and protease inhibitors cocktail [Roche]). GTP-bound Cdc42 was affinity purified using GST-PAK-CRIB attached to glutathione Sepharose beads (GE Healthcare). Proteins were eluted with SDS sample buffer and analyzed by 15% SDS-PAGE and anti-Cdc42 Western blotting.

### Online supplemental material

Fig. S1 shows the depletion of Arf6 by siRNA and its consequences on Golgi structure, focal adhesion localization, and cell migration. Fig. S2 shows that Cdc42 localization at the leading edge is independent of Rac activity. Fig. S3 shows that Arf6 and βPIX are involved in Rac recruitment to the leading edge. Videos 1–3 and 5 show spinning-disc imaging of GFP-Cdc42 dynamics in migrating (Videos 1 and 2), nonmigrating (Video 3), and Arf6-depleted astrocytes (Video 5). Video 4 shows phase-contrast images of membrane dynamics at the leading edge of migrating astrocytes. Videos 6 and 7 show phase-contrast images of control and Arf6-depleted astrocytes. Online supplemental material is available at <http://www.jcb.org/cgi/content/full/jcb.201003091/DC1>.

We thank Inke Näthke, Nicolas Vitale, and W.M. Bement for reagents and constructs and the Imaging Platform at Institut Pasteur for technical help.

This work was supported by the Agence Nationale de la Recherche, the Institut Pasteur, and La Ligue contre le Cancer. N. Osmani is funded by the Association pour la Recherche sur le Cancer. S. Etienne-Manneville is a member of the European Molecular Biology Organization Young Investigator Programme.

Submitted: 19 March 2010

Accepted: 22 November 2010

## References

Adams, A.E., D.I. Johnson, R.M. Longnecker, B.F. Sloat, and J.R. Pringle. 1990. CDC42 and CDC43, two additional genes involved in budding and the establishment of cell polarity in the yeast *Saccharomyces cerevisiae*. *J. Cell Biol.* 111:131–142. doi:10.1083/jcb.111.1.131

Albertinazzi, C., L. Za, S. Paris, and I. de Curtis. 2003. ADP-ribosylation factor 6 and a functional PIX/p95-APP1 complex are required for Rac1B-mediated neurite outgrowth. *Mol. Biol. Cell.* 14:1295–1307. doi:10.1091/mbc.E02-07-0406

Allen, W.E., D. Zicha, A.J. Ridley, and G.E. Jones. 1998. A role for Cdc42 in macrophage chemotaxis. *J. Cell Biol.* 141:1147–1157. doi:10.1083/jcb.141.5.1147

Balasubramanian, N., D.W. Scott, J.D. Castle, J.E. Casanova, and M.A. Schwartz. 2007. Arf6 and microtubules in adhesion-dependent trafficking of lipid rafts. *Nat. Cell Biol.* 9:1381–1391. doi:10.1038/ncb1657

Cau, J., and A. Hall. 2005. Cdc42 controls the polarity of the actin and microtubule cytoskeletons through two distinct signal transduction pathways. *J. Cell Sci.* 118:2579–2587. doi:10.1242/jcs.02385

Caviston, J.P., S.E. Tcheperegine, and E. Bi. 2002. Singularity in budding: a role for the evolutionarily conserved small GTPase Cdc42p. *Proc. Natl. Acad. Sci. USA.* 99:12185–12190. doi:10.1073/pnas.182370299

Cotton, M., P.L. Boulay, T. Houndolo, N. Vitale, J.A. Pitcher, and A. Claing. 2007. Endogenous ARF6 interacts with Rac1 upon angiotensin II stimulation to regulate membrane ruffling and cell migration. *Mol. Biol. Cell.* 18:501–511. doi:10.1091/mbc.E06-06-0567

D'Souza-Schorey, C., and P. Chavrier. 2006. ARF proteins: roles in membrane traffic and beyond. *Nat. Rev. Mol. Cell Biol.* 7:347–358. doi:10.1038/nrm1910

D'Souza-Schorey, C., E. van Donselaar, V.W. Hsu, C. Yang, P.D. Stahl, and P.J. Peters. 1998. ARF6 targets recycling vesicles to the plasma membrane:

insights from an ultrastructural investigation. *J. Cell Biol.* 140:603–616. doi:10.1083/jcb.140.3.603

Daher, Z., J. Noël, and A. Claing. 2008. Endothelin-1 promotes migration of endothelial cells through the activation of ARF6 and the regulation of FAK activity. *Cell. Signal.* 20:2256–2265. doi:10.1016/j.cellsig.2008.08.021

Di Cesare, A., S. Paris, C. Albertinazzi, S. Dariozzi, J. Andersen, M. Mann, R. Longhi, and I. de Curtis. 2000. p95-APP1 links membrane transport to Rac-mediated reorganization of actin. *Nat. Cell Biol.* 2:521–530. doi:10.1038/35019561

Erickson, J.W., C. Zhang, R.A. Kahn, T. Evans, and R.A. Cerione. 1996. Mammalian Cdc42 is a brefeldin A-sensitive component of the Golgi apparatus. *J. Biol. Chem.* 271:26850–26854. doi:10.1074/jbc.271.43.26850

Etienne-Manneville, S. 2004. Cdc42—the centre of polarity. *J. Cell Sci.* 117:1291–1300. doi:10.1242/jcs.01115

Etienne-Manneville, S. 2006. In vitro assay of primary astrocyte migration as a tool to study Rho GTPase function in cell polarization. *Methods Enzymol.* 406:565–578. doi:10.1016/S0076-6879(06)06044-7

Etienne-Manneville, S., and A. Hall. 2001. Integrin-mediated activation of Cdc42 controls cell polarity in migrating astrocytes through PKCzeta. *Cell.* 106:489–498. doi:10.1016/S0092-8674(01)00471-8

Etienne-Manneville, S., and A. Hall. 2002. Rho GTPases in cell biology. *Nature.* 420:629–635. doi:10.1038/nature01148

Etienne-Manneville, S., and A. Hall. 2003. Cdc42 regulates GSK-3beta and adenomatous polyposis coli to control cell polarity. *Nature.* 421:753–756. doi:10.1038/nature01423

Etienne-Manneville, S., J.B. Manneville, S. Nicholls, M.A. Ferenczi, and A. Hall. 2005. Cdc42 and Par6–PKCζ regulate the spatially localized association of Dlg1 and APC to control cell polarization. *J. Cell Biol.* 170:895–901. doi:10.1083/jcb.200412172

Farooqui, R., S. Zhu, and G. Fenteany. 2006. Glycogen synthase kinase-3 acts upstream of ADP-ribosylation factor 6 and Rac1 to regulate epithelial cell migration. *Exp. Cell Res.* 312:1514–1525. doi:10.1016/j.yexcr.2006.01.018

Feng, Q., D. Baird, X. Peng, J. Wang, T. Ly, J.L. Guan, and R.A. Cerione. 2006. Cool-1 functions as an essential regulatory node for EGF receptor- and Src-mediated cell growth. *Nat. Cell Biol.* 8:945–956. doi:10.1038/ncb1453

Georgiou, M., E. Marinari, J. Burden, and B. Baum. 2008. Cdc42, Par6, and aPKC regulate Arp2/3-mediated endocytosis to control local adherens junction stability. *Curr. Biol.* 18:1631–1638. doi:10.1016/j.cub.2008.09.029

Hehny, H., K.M. Longhini, J.L. Chen, and M. Stamnes. 2009. Retrograde Shiga toxin trafficking is regulated by ARHGAP21 and Cdc42. *Mol. Biol. Cell.* 20:4303–4312. doi:10.1091/mbc.E09-02-0155

Hoefen, R.J., and B.C. Berk. 2006. The multifunctional GIT family of proteins. *J. Cell Sci.* 119:1469–1475. doi:10.1242/jcs.02925

Hu, B., B. Shi, M.J. Jarzynka, J.J. Yiin, C. D'Souza-Schorey, and S.Y. Cheng. 2009. ADP-ribosylation factor 6 regulates glioma cell invasion through the IQ-domain GTPase-activating protein 1-Rac1-mediated pathway. *Cancer Res.* 69:794–801. doi:10.1158/0008-5472.CAN-08-2110

Johnson, D.I. 1999. Cdc42: an essential Rho-type GTPase controlling eukaryotic cell polarity. *Microbiol. Mol. Biol. Rev.* 63:54–105.

Li, Z., M. Hannigan, Z. Mo, B. Liu, W. Lu, Y. Wu, A.V. Smrcka, G. Wu, L. Li, M. Liu, et al. 2003. Directional sensing requires G beta gamma-mediated PAK1 and PIX alpha-dependent activation of Cdc42. *Cell.* 114:215–227. doi:10.1016/S0092-8674(03)00559-2

Li, M., S.S. Ng, J. Wang, L. Lai, S.Y. Leung, M. Franco, Y. Peng, M.L. He, H.F. Kung, and M.C. Lin. 2006. EFA6A enhances glioma cell invasion through ADP ribosylation factor 6/extracellular signal-regulated kinase signaling. *Cancer Res.* 66:1583–1590. doi:10.1158/0008-5472.CAN-05-2424

Manneville, J.B., M. Jehanno, and S. Etienne-Manneville. 2010. Dlg1 binds GKAP to control dynein association with microtubules, centrosome positioning, and cell polarity. *J. Cell Biol.* 191:585–598. doi:10.1083/jcb.201002151

Matafora, V., S. Paris, S. Dariozzi, and I. de Curtis. 2001. Molecular mechanisms regulating the subcellular localization of p95-APP1 between the endosomal recycling compartment and sites of actin organization at the cell surface. *J. Cell Sci.* 114:4509–4520.

Michaelson, D., J. Silletti, G. Murphy, P. D'Eustachio, M. Rush, and M.R. Philips. 2001. Differential localization of Rho GTPases in live cells: regulation by hypervariable regions and RhoGDI binding. *J. Cell Biol.* 152:111–126. doi:10.1083/jcb.152.1.111

Mott, H.R., D. Nietlispach, K.A. Evetts, and D. Owen. 2005. Structural analysis of the SH3 domain of beta-PIX and its interaction with alpha-p21 activated kinase (PAK). *Biochemistry.* 44:10977–10983. doi:10.1021/bi050374a

Nalbant, P., L. Hodgson, V. Kraynov, A. Touchkine, and K.M. Hahn. 2004. Activation of endogenous Cdc42 visualized in living cells. *Science.* 305:1615–1619. doi:10.1126/science.1100367

- Nern, A., and R.A. Arkowitz. 2000. Nucleocytoplasmic shuttling of the Cdc42p exchange factor Cdc24p. *J. Cell Biol.* 148:1115–1122. doi:10.1083/jcb.148.6.1115
- Nobes, C., and M. Marsh. 2000. Dendritic cells: new roles for Cdc42 and Rac in antigen uptake? *Curr. Biol.* 10:R739–R741. doi:10.1016/S0960-9822(00)00736-3
- Osmani, N., N. Vitale, J.P. Borg, and S. Etienne-Manneville. 2006. Scrib controls Cdc42 localization and activity to promote cell polarization during astrocyte migration. *Curr. Biol.* 16:2395–2405. doi:10.1016/j.cub.2006.10.026
- Palacios, F., and C. D'Souza-Schorey. 2003. Modulation of Rac1 and ARF6 activation during epithelial cell scattering. *J. Biol. Chem.* 278:17395–17400. doi:10.1074/jbc.M300998200
- Palazzo, A.F., T.A. Cook, A.S. Alberts, and G.G. Gundersen. 2001. mDia mediates Rho-regulated formation and orientation of stable microtubules. *Nat. Cell Biol.* 3:723–729. doi:10.1038/35087035
- Park, H.O., and E. Bi. 2007. Central roles of small GTPases in the development of cell polarity in yeast and beyond. *Microbiol. Mol. Biol. Rev.* 71:48–96. doi:10.1128/MMBR.00028-06
- Pegtel, D.M., S.I. Ellenbroek, A.E. Mertens, R.A. van der Kammen, J. de Rooij, and J.G. Collard. 2007. The Par-Tiam1 complex controls persistent migration by stabilizing microtubule-dependent front-rear polarity. *Curr. Biol.* 17:1623–1634. doi:10.1016/j.cub.2007.08.035
- Peters, P.J., V.W. Hsu, C.E. Ooi, D. Finazzi, S.B. Teal, V. Oorschot, J.G. Donaldson, and R.D. Klausner. 1995. Overexpression of wild-type and mutant ARF1 and ARF6: distinct perturbations of nonoverlapping membrane compartments. *J. Cell Biol.* 128:1003–1017. doi:10.1083/jcb.128.6.1003
- Radhakrishna, H., and J.G. Donaldson. 1997. ADP-ribosylation factor 6 regulates a novel plasma membrane recycling pathway. *J. Cell Biol.* 139:49–61. doi:10.1083/jcb.139.1.49
- Rodal, A.A., R.N. Motola-Barnes, and J.T. Littleton. 2008. Nervous wreck and Cdc42 cooperate to regulate endocytic actin assembly during synaptic growth. *J. Neurosci.* 28:8316–8325. doi:10.1523/JNEUROSCI.2304-08.2008
- Sabe, H. 2003. Requirement for Arf6 in cell adhesion, migration, and cancer cell invasion. *J. Biochem.* 134:485–489. doi:10.1093/jb/mvg181
- Santy, L.C., and J.E. Casanova. 2001. Activation of ARF6 by ARNO stimulates epithelial cell migration through downstream activation of both Rac1 and phospholipase D. *J. Cell Biol.* 154:599–610. doi:10.1083/jcb.200104019
- Santy, L.C., K.S. Ravichandran, and J.E. Casanova. 2005. The DOCK180/Elmo complex couples ARNO-mediated Arf6 activation to the downstream activation of Rac1. *Curr. Biol.* 15:1749–1754. doi:10.1016/j.cub.2005.08.052
- Shimada, Y., M.P. Gullii, and M. Peter. 2000. Nuclear sequestration of the exchange factor Cdc24 by Far1 regulates cell polarity during yeast mating. *Nat. Cell Biol.* 2:117–124. doi:10.1038/35000073
- Slaughter, B.D., A. Das, J.W. Schwartz, B. Rubinstein, and R. Li. 2009. Dual modes of cdc42 recycling fine-tune polarized morphogenesis. *Dev. Cell.* 17:823–835. doi:10.1016/j.devcel.2009.10.022
- Svensson, H.G., M.A. West, P. Mollahan, A.R. Prescott, R. Zaru, and C. Watts. 2008. A role for ARF6 in dendritic cell podosome formation and migration. *Eur. J. Immunol.* 38:818–828. doi:10.1002/eji.200737331
- ten Klooster, J.P., Z.M. Jaffer, J. Chernoff, and P.L. Hordijk. 2006. Targeting and activation of Rac1 are mediated by the exchange factor  $\beta$ -Pix. *J. Cell Biol.* 172:759–769. doi:10.1083/jcb.200509096
- Torii, T., Y. Miyamoto, A. Sanbe, K. Nishimura, J. Yamauchi, and A. Tanoue. 2010. Cytohesin-2/ARNO, through its interaction with focal adhesion adaptor protein paxillin, regulates preadipocyte migration via the downstream activation of Arf6. *J. Biol. Chem.* 285:24270–24281. doi:10.1074/jbc.M110.125658
- Wedlich-Soldner, R., S. Altschuler, L. Wu, and R. Li. 2003. Spontaneous cell polarization through actomyosin-based delivery of the Cdc42 GTPase. *Science.* 299:1231–1235. doi:10.1126/science.1080944
- Wedlich-Soldner, R., S.C. Wai, T. Schmidt, and R. Li. 2004. Robust cell polarity is a dynamic state established by coupling transport and GTPase signaling. *J. Cell Biol.* 166:889–900. doi:10.1083/jcb.200405061
- Wu, W.J., J.W. Erickson, R. Lin, and R.A. Cerione. 2000. The gamma-subunit of the coatomer complex binds Cdc42 to mediate transformation. *Nature.* 405:800–804. doi:10.1038/35015585